Cannabinoid CB_2 receptors modulate midbrain dopamine neuronal activity and dopamine-related behavior in mice

Hai-Ying Zhang[a,1], Ming Gao[b,1], Qing-Rong Liu[a], Guo-Hua Bi[a], Xia Li[c], Hong-Ju Yang[a], Eliot L. Gardner[a], Jie Wu[b,d,e,2], and Zheng-Xiong Xi[a,2]

[a]Intramural Research Program, National Institute on Drug Abuse, Baltimore, MD 21224; [b]Divisions of Neurology and Neurobiology, Barrow Neurological Institute, St. Joseph's Hospital and Medical Center, Phoenix, AZ 85013; [c]Department of Psychiatry, School of Medicine, University of California, San Diego, La Jolla, CA 92093; [d]Department of Basic Medical Sciences, University of Arizona College of Medicine, Phoenix, AZ 85004; and [e]Department of Physiology, Shantou University Medical College, Shantou, Guangdong 210854, China

Edited by Leslie Lars Iversen, University of Oxford, Oxford, United Kingdom, and approved October 6, 2014 (received for review July 11, 2014)

Cannabinoid CB_2 receptors (CB_2Rs) have been recently reported to modulate brain dopamine (DA)-related behaviors; however, the cellular mechanisms underlying these actions are unclear. Here we report that CB_2Rs are expressed in ventral tegmental area (VTA) DA neurons and functionally modulate DA neuronal excitability and DA-related behavior. In situ hybridization and immunohistochemical assays detected CB_2 mRNA and CB_2R immunostaining in VTA DA neurons. Electrophysiological studies demonstrated that activation of CB_2Rs by JWH133 or other CB_2R agonists inhibited VTA DA neuronal firing in vivo and ex vivo, whereas microinjections of JWH133 into the VTA inhibited cocaine self-administration. Importantly, all of the above findings observed in WT or $CB_1^{-/-}$ mice are blocked by CB_2R antagonist and absent in $CB_2^{-/-}$ mice. These data suggest that CB_2R-mediated reduction of VTA DA neuronal activity may underlie JWH133's modulation of DA-regulated behaviors.

cannabinoid | CB_2 receptor | JWH133 | dopamine | cocaine

The presence of functional cannabinoid CB_2 receptors (CB_2Rs) in the brain has been controversial. When CB_2Rs were first cloned, in situ hybridization (ISH) failed to detect CB_2 mRNA in brain (1). Similarly, Northern blot and polymerase chain reaction (PCR) assays failed to detect CB_2 mRNA in brain (2–5). Therefore, CB_2Rs were considered "peripheral cannabinoid receptors" (1, 6).

In contrast, other studies using ISH and radioligand binding assays detected CB_2 mRNA and receptor binding in rat retina (7), mouse cerebral cortex (8), and hippocampus and striatum of nonhuman primates (9). More recent studies using RT-PCR also detected CB_2 mRNA in the cortex, striatum, hippocampus, amygdala, and brainstem (9–14). Immunoblot and immunohistochemistry (IHC) assays detected CB_2R immunoreactivity or immunostaining in various brain regions (13, 15–20). The specificities of the detected CB_2R protein and CB_2-mRNA remain questionable, however, owing to a lack of controls using $CB_1^{-/-}$ and $CB_2^{-/-}$ mice in most previous studies (21). A currently accepted view is that brain CB_2Rs are expressed predominantly in activated microglia during neuroinflammation, whereas brain neurons, except for a very small number in the brainstem, lack CB_2R expression (21).

On the other hand, we recently reported that brain CB_2Rs modulate cocaine self-administration and cocaine-induced increases in locomotion and extracellular dopamine (DA) in the nucleus accumbens in mice (22). This finding is supported by recent studies demonstrating that systemic administration of the CB_2R agonist O-1966 inhibited cocaine-induced conditioned place preference in WT mice, but not in $CB_2^{-/-}$ mice (23), and that increased CB_2R expression in mouse brain attenuates cocaine self-administration and cocaine-enhanced locomotion (19). In addition, brain CB_2Rs may be involved in several DA-related CNS disorders, such as Parkinson's disease (24), schizophrenia (25), anxiety (26), and depression (27). The cellular mechanisms underlying CB_2R modulation of DA-related behaviors and diseases are unclear, however. Given that midbrain DA neurons of the ventral tegmental area (VTA) play an important role in mediating the reinforcing and addictive effects of drugs of abuse (28, 29), we hypothesized that brain CB_2Rs, similar to other G protein-coupled receptors, are expressed in VTA DA neurons, where they modulate DA neuronal function and DA-related behaviors.

In the present study, we tested this hypothesis using multiple approaches. We first assayed for CB_2 mRNA and protein expression in brain and in VTA DA neurons using quantitative RT-PCR (qRT-PCR), ISH, and double-label IHC techniques. We then examined the effects of the selective CB_2R agonist JWH133 and several other CB_2R agonists on VTA DA neuronal firing in both ex vivo and in vivo preparations using electrophysiological methods. Finally, we observed the effects of microinjections of JWH133 into the VTA on intravenous cocaine self-administration to study whether activation of VTA CB_2Rs modulates DA-dependent behavior. This multidisciplinary approach has provided evidence of functional CB_2Rs in VTA DA neurons. Importantly, all findings observed in WT or $CB_1^{-/-}$ mice

Significance

Although early studies suggested that cannabinoid CB_2 receptors (CB_2Rs) are absent in the brain, this view has been challenged by recent findings of significant brain CB_2R involvement in several dopamine (DA)-related CNS disorders. The cellular mechanisms underlying these actions are unclear, however. Using multiple approaches, we found that CB_2R genes and receptors are expressed in midbrain DA neurons, and that activation of CB_2Rs inhibits DA neuronal firing and i.v. cocaine self-administration. These findings not only challenge the long-held view that brain CB_2Rs are not expressed in neurons, but also suggest that neuronal CB_2Rs modulate DA neuronal activity and DA-regulated behavior. Thus, brain CB_2Rs may constitute a new therapeutic target in medication development for treatment of a number of CNS disorders.

Author contributions: H.-Y.Z., M.G., Q.-R.L., E.L.G., J.W., and Z.-X.X. designed research; H.-Y.Z., M.G., G.-H.B., X.L., H.-J.Y., and J.W. performed research; H.-Y.Z., M.G., G.-H.B., X.L., H.-J.Y., J.W., and Z.-X.X. analyzed data; and H.-Y.Z., E.L.G., J.W., and Z.-X.X. wrote the paper.

The authors declare no conflict of interest.

This article is a PNAS Direct Submission.

Freely available online through the PNAS open access option.

[1]H.-Y.Z. and M.G. contributed equally to this work.

[2]To whom correspondence may be addressed. Email: zxi@intra.nida.nih.gov or jie.wu@dignityhealth.org.

This article contains supporting information online at www.pnas.org/lookup/suppl/doi:10.1073/pnas.1413210111/-/DCSupplemental.

were blocked by a CB_2R antagonist and/or absent in $CB_2^{-/-}$ mice, suggesting that CB_2Rs expressed in VTA DA neurons play an important role in modulating DA neuronal activity and DA-related functions.

Results

CB_2 mRNA Is Expressed in the Brain. We first used qRT-PCR to examine CB_2 mRNA expression in the brain and spleen of WT, $CB_1^{-/-}$, and $CB_2^{-/-}$ mice using three different TaqMan probes targeting different gene sequences (Fig. 1 and Table S1). Fig. 1 shows the gene structure, two mouse CB_2R transcripts (CB_{2A} and CB_{2B}), the CB_2 gene-deleted region in $CB_2^{-/-}$ mice (6), and three probes used to detect CB_2 mRNA in WT, $CB_1^{-/-}$, and $CB_2^{-/-}$ mice. When using the probes that target the conjunction region of exons 1 and 3 (CB_{2A} probe) or exons 2 and 3 (CB_{2B} probe), we detected similar or even higher levels of CB_{2A} and CB_{2B} mRNA in prefrontal cortex, striatum, midbrain, and spleen in $CB_2^{-/-}$ mice compared with WT mice (Fig. 1*C*, *Left* and *Middle*); however, when using the CB_2-KO probe that targets the deleted gene sequence in $CB_2^{-/-}$ mice (Fig. 1*B*), we detected CB_2 mRNA in WT and $CB_1^{-/-}$ mice, but not in $CB_2^{-/-}$ mice (Fig. 1*C*, *Right*). Further quantitative assays indicated that CB_{2A} mRNA was ∼60 times lower in cortex than in spleen (Fig. 1*C*, *Left*), and that CB_{2B} mRNA was ∼500 times lower in cortex than in spleen (Fig. 1*C*, *Middle*).

CB_2 mRNA Is Expressed in VTA DA Neurons. Based on the foregoing findings, we successfully developed a CB_2-specific riboprobe targeting the gene-deleted regions in the presently used $CB_2^{-/-}$ mice to examine CB_2 mRNA expression in VTA DA neurons. In this experiment, we first used traditional ISH methods (*SI Experimental Procedures*) to examine CB_2 mRNA in VTA neurons, and then performed IHC assays with tyrosine hydroxylase (TH) antibody to identify the phenotype(s) of CB_2 mRNA-positive neurons. We found that the antisense riboprobe detected CB_2 mRNA signaling in the midbrain of WT and $CB_1^{-/-}$ mice, but not $CB_2^{-/-}$ mice (Fig. 2 *A*, *b*), and that the corresponding CB_2-mRNA sense (control) probe did not detect any mRNA signal (Fig. 2 *A*, *b*). Fig. 2 *A*, *c* shows representative ISH-IHC images in the VTA, illustrating detection of CB_2 mRNA staining in VTA DA neurons (TH-positive) in WT mice, but not in $CB_2^{-/-}$ mice, suggesting that CB_2R mRNA is expressed in VTA DA neurons.

To confirm this finding, we used another highly-sensitive RNAscope ISH method, which allowed us to simultaneously detect TH mRNA and CB_2 mRNA in VTA neurons. In this experiment, we initially designed two RNAscope probes that target the deleted gene sequences in $CB_2^{-/-}$ mice and the 3′ untranslated region (UTR) of the CB_2 gene, respectively. We found only one probe targeting the 3′ UTR (Fig. 2 *B*, *a*) that worked well. Fig. 2 *B*, *b* and *c* shows CB_2 mRNA staining in VTA DA (TH mRNA-positive) neurons in WT and $CB_2^{-/-}$ mice using this RNAscope probe. This probe apparently detected CB_2 mRNA in $CB_2^{-/-}$ mice, because it detected the intact 3′ UTR region located downstream of the gene-deleted sequence (Fig. 2 *B*, *a*). Fig. S1 shows representative confocal images under high magnification, illustrating colocalization of CB_2 mRNA with TH mRNA in VTA DA neurons of WT and $CB_2^{-/-}$ mice. In addition, CB_2 mRNA is also expressed in TH-negative VTA non-DA neurons (Fig. S1). Taken together, the

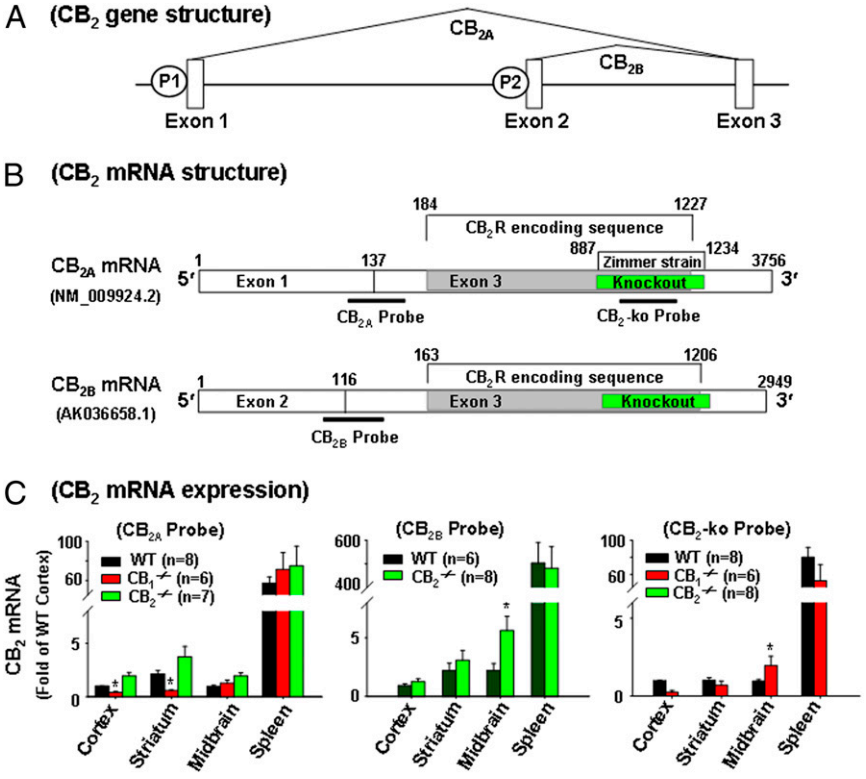

Fig. 1. CB_2 mRNA expression in WT, $CB_1^{-/-}$, and $CB_2^{-/-}$ mice. (*A*) Mouse CB_2 genomic structure and transcripts (mRNAs), illustrating that the CB_2 gene contains three exons with two separate promoters (P1 and P2). (*B*) CB_{2A} and CB_{2B} transcripts and the binding sites of three TaqMan probes used to detect CB_2 mRNA by RT-PCR. The CB_{2A} and CB_{2B} probes target the 5′ UTR, whereas the CB_2-KO probe targets the CB_2-deleted gene sequence in the Zimmer strain of $CB_2^{-/-}$ mice. (*C*) CB_2 mRNA was detectable in WT, $CB_1^{-/-}$, and $CB_2^{-/-}$ mice when using the CB_{2A} or CB_{2B} probe, but was not detectable in $CB_2^{-/-}$ mice when using the CB_2-KO probe. The CB_2 mRNA levels in each brain or spleen tissue are the relative levels (folds) compared with those in cortex of WT mice (defined as 1). All quantificated data are normalized to control (cortex). Error bars indicate ±SEM. *$P < 0.05$, compared with WT mice. NM_009924.2 and AK036658.1 are the GenBank cDNA codes.

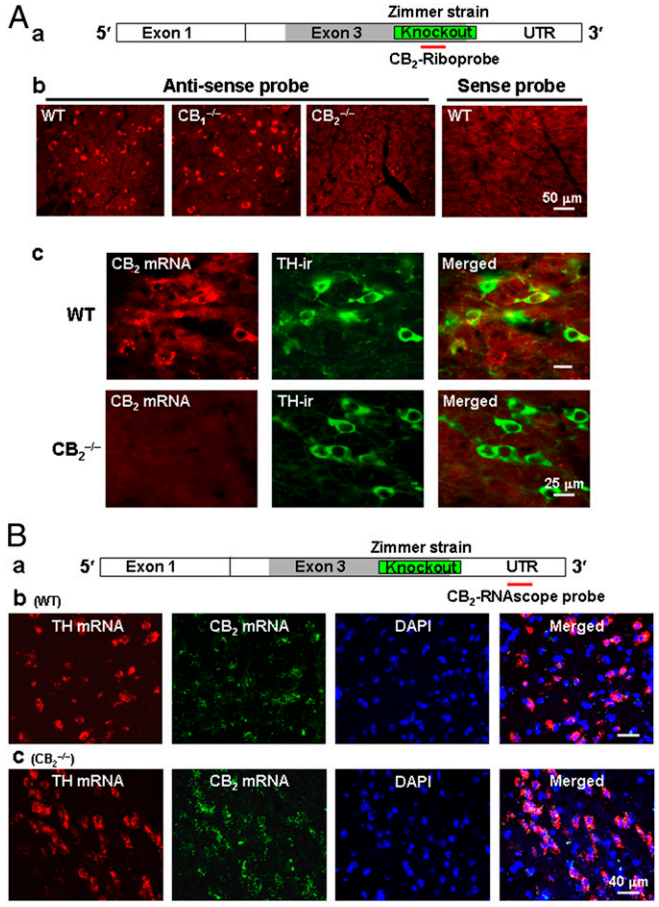

Fig. 2. CB_2 mRNA expression in VTA DA neurons by ISH assays. (*A*, *a*) CB_{2A} mRNA and the location detected by a CB_2-riboprobe. (*A*, *b*) The antisense, but not the sense (control), riboprobe detected CB_2 mRNA in midbrain neurons in WT and $CB_1^{-/-}$ mice, but not in $CB_2^{-/-}$ mice. (*A*, *c*) Double-label fluorescent images of CB_2 mRNA (by ISH) and TH (by IHC) staining, illustrating CB_2 mRNA staining in individual TH-positive VTA DA neurons in WT mice, but not in $CB_2^{-/-}$ mice (Zimmer strain). (*B*, *a*) CB_{2A} mRNA and the location detected by a CB_2-RNAscope probe. (*B*, *b* and *c*) CB_2-RNAscope probe-detected CB_2 mRNA in VTA DA neurons in WT and $CB_2^{-/-}$ mice. This probe detected CB_2 mRNA in $CB_2^{-/-}$ mice because it targets the downstream UTR region rather than the upstream gene-deleted region. Scales are shown in the figures. Also see Fig. S1.

two different ISH assays with two probes targeting different gene sequences detected similar CB_2 mRNA staining in VTA DA neurons, suggesting that the $CB_2^{-/-}$ mice used in this study (Zimmer strain) are partial knockouts, and that the majority of the upstream and downstream gene sequences from the gene-deleted region are still present in this strain of $CB_2^{-/-}$ mice.

CB_2R Immunostaining Is Detected in VTA DA Neurons. After detecting CB_2 mRNA, we assayed for CB_2R protein expression in VTA DA neurons using IHC techniques. Fig. S2*A* shows the mouse CB_2R structures in WT and $CB_2^{-/-}$ mice, the deleted receptor region in $CB_2^{-/-}$ mice, and the binding sites (epitopes) of three antibodies on mouse CB_2Rs. Fig. S2*B* shows representative mouse CB_2 immunostaining with the NIH-5633 mouse CB_2 (mCB_2) antibody under various magnifications (4×, 10×, 20×, and 40×) in the midbrain of WT mice, illustrating CB_2 immunostaining in VTA DA neurons (labeled by TH; yellow in merged images), as well as in VTA non-DA cells (green cells in merged images). Fig. S3 shows representative CB_2 immunostaining with the Abcam rCB_2 Ab that recognizes the intact N terminal of CB_2Rs in $CB_2^{-/-}$ mice, illustrating similar densities of CB_2 immunostaining in VTA DA neurons in WT, $CB_1^{-/-}$, and $CB_2^{-/-}$ mice.

Fig. 3 *A* and *B* presents representative confocal images of mCB_2R immunostaining using the NIH-5633 and Alomone mCB_2 antibodies that target the deleted intracellular third loop or the deleted C terminal of CB_2Rs in $CB_2^{-/-}$ mice, illustrating that CB_2R staining was detected in VTA DA neurons in WT and $CB_1^{-/-}$ mice, but barely detectable in $CB_2^{-/-}$ mice. Preabsorption of the antibody with specific immune peptide blocked CB_2R immunostaining in VTA DA neurons, suggesting that both antibodies are mCB_2-specific. Fig. 3 *C* and *D* shows mean densities of CB_2R immunostaining per DA neuron over hundreds of TH-positive DA neurons from two to five WT, $CB_1^{-/-}$, or $CB_2^{-/-}$ mice, illustrating a significant reduction in the density of CB_2R immunostaining in DA neurons in $CB_2^{-/-}$ mice compared with WT mice (Fig. 3*C*: $F_{2,1067} = 142.42$, $P < 0.001$; Fig. 3*D*: $F_{2,669} = 235.50$, $P < 0.001$). These findings suggest that (*i*) the presently used $CB_2^{-/-}$ strain is a partial CB_2 knockout mouse, (*ii*) both the NIH-5633 and Alomone mCB_2 antibodies display a significant degree of (but not absolute) mCB_2R specificity, and (*iii*) the Abcam rCB_2 antibody specificity is unknown, because N terminal-containing CB_2R fragment(s) may be present in this strain of $CB_2^{-/-}$ mice.

CB_2R Immunostaining Is Detected in Splenocytes, but Is Barely Detectable in Glial Cells. We also used the same antibodies to detect CB_2 immunostaining in CB_2-rich splenocytes. Fig. S4 shows that both the NIH-5633 and Alomone antibodies detected high densities of CB_2 immunostaining in splenocytes of WT mice, but very low densities in $CB_2^{-/-}$ mice. Finally, we used the

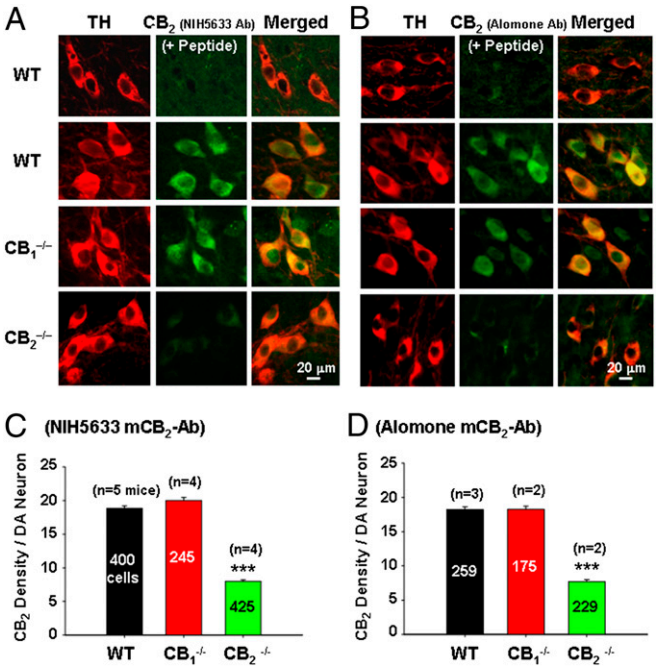

Fig. 3. Mouse CB_2 immunostaining in VTA DA neurons. (*A* and *B*) Representative confocal images of CB_2R immunostaining in VTA DA neurons, illustrating that the NIH-5633 (*A*) and Alomone (*B*) mCB_2 antibodies (with epitopes in the deleted portion of the receptor in Zimmer $CB_2^{-/-}$ mice) were detected by CB_2 immunostaining in VTA DA neurons in WT and $CB_1^{-/-}$ mice, but were barely detectable in $CB_2^{-/-}$ mice. Preabsorption of the antibody by specific immune peptide blocked CB_2R immunostaining. (*C* and *D*) Mean densities of CB_2R immunostaining in VTA DA neurons of WT, $CB_1^{-/-}$, and $CB_2^{-/-}$ mice. The numbers in the graph bars are numbers of TH-positive VTA DA neurons. All quantificated data are means ± SEM. ***$P < 0.001$, compared with WT mice. Also see Figs. S2–S5.

same antibodies to determine whether CB_2 receptors are expressed in glial cells. Fig. S5 shows that the NIH-5633 antibody detected a very low density of CB_2 immunostaining in GFAP-labeled astrocytes, but not in CD11b-labeled microglia, in mice treated with vehicle (saline) or lipopolysaccharide (LPS), a bacterial endotoxin. These data suggest that CB_2Rs are expressed mainly in DA neurons rather than in glial cells in the VTA.

CB_2Rs Modulate Neuronal Firing in Single Dissociated VTA DA Neurons. None of the foregoing tested antibodies was completely mCB_2-specific; thus, we next used electrophysiological methods to examine whether CB_2Rs in VTA DA neurons are functionally responsive to CB_2R ligands. We first examined the effects of the selective CB_2R agonist JWH133 on DA neuronal firing using perforated patch-clamp recording in single dissociated VTA DA neurons. Identification of DA neurons was based on three criteria (30, 31): electrophysiology [DA neurons exhibit low spontaneous firing rates (FRs; 1–3 Hz) with long action potential (AP) duration and a distinctive H-current], pharmacology [DA neuronal firing is inhibited by DA or by a D_2 receptor agonist (e.g., quinpirole)], and IHC staining (recorded neurons are TH-positive) (Fig. S6).

Fig. 4 shows a representative dissociated TH-positive VTA DA neuron (Fig. 4*A*) and characteristic low DA neuronal FR (~1 Hz) (Fig. 4*B*). JWH133 significantly reduced VTA DA neuronal firing in WT mice in a dose-dependent manner (Fig. 4 *B* and *C*, *a*; $^{**}P < 0.01$, paired *t* test, compared with pre-JWH133 baseline). This effect was blocked by coadministration of the selective CB_2R antagonist AM630 (1 μM) and was absent in $CB_2^{-/-}$ mice (Fig. 4 *C*, *a*). AM630 alone (1 μM) did not affect neuronal firing. In addition, we also tested the effects of four additional CB_2R agonists [GW405833 (GW), SER601, CB65, and HU308] on VTA DA neuronal firing, and found that all tested CB_2R agonists produced similar inhibitory effects on DA neuronal firing (Fig. 4 *C*, *b*) ($^{*}P < 0.05$, paired *t* tests).

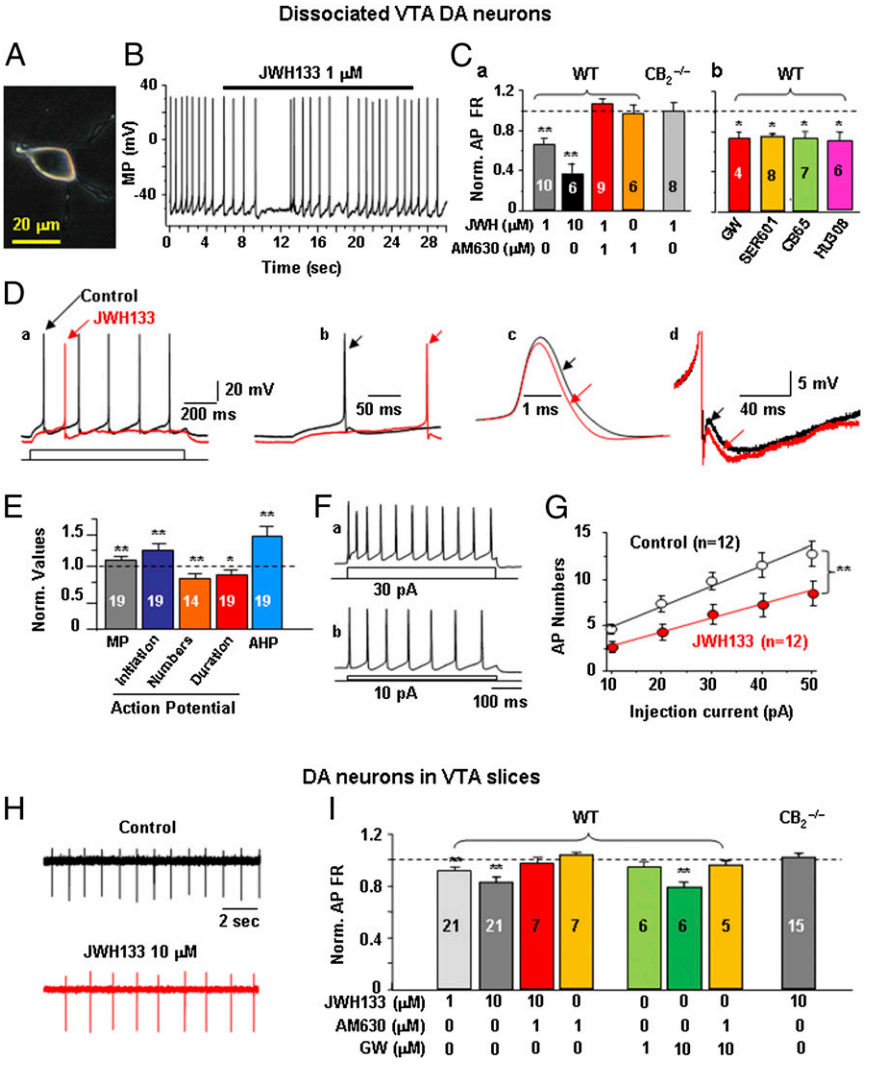

Fig. 4. Activation of CB_2Rs reduces VTA DA neuronal firing ex vivo. (*A*) Phase-photo image showing a dissociated VTA DA neuron. (*B* and *C*) Representative recording and summarized data illustrating that JWH133 and additional four CB_2R agonists (GW405833, SER601, CB65, and HU308) inhibited VTA DA neuronal firing similarly in WT mice, but not in Zimmer $CB_2^{-/-}$ mice. This inhibitory effect was blocked by coadministration of AM630 (1 μM). (*D* and *E*) Representative AP traces and summarized group data illustrating that JWH133 altered membrane potential (MP), AP firing rate, AP initiation, AP duration, and AHP in WT mice. (*F* and *G*) Representative depolarizing current-induced AP firing and summarized data illustrating that JWH133 decreased VTA DA neuronal excitability. (*H* and *I*) Representative records and summarized data illustrating that JWH133 or GW405833 (GW) inhibited VTA DA neuronal firing in brain slices in a concentration-dependent manner. This effect was blocked by coadministration of AM630 and was absent in $CB_2^{-/-}$ mice. All quantificated data are normalized to control (predrug baseline). Error bars indicate ± SEM. $^{*}P < 0.05$; $^{**}P < 0.01$, compared with predrug controls. Also see Fig. S6.

Further analysis of neuronal firing patterns revealed that JWH133 significantly attenuated the AP FR (Fig. 4 *D*, *a*), hyperpolarized the membrane potential (Fig. 4 *D*, *b*), prolonged AP initiation latency (Fig. 4 *D*, *b*), shortened AP duration (Fig. 4 *D*, *c*), and increased the afterhyperpolarization potential (AHP) (Fig. 4 *D*, *d*). Fig. 4*E* shows pooled data, illustrating that JWH133-induced changes in each AP parameter were statistically significant compared with pre-JWH133 baselines (*$P < 0.05$; **$P < 0.01$, paired *t* tests). The actual values of each AP parameter before and after JWH133 administration are presented in Table S2. Fig. 4 *F* and *G* shows AP firing induced by injections of different intensities of current (10–50 pA) via the recording electrode, illustrating that JWH133 (1 μM) significantly shifted the input–output relationship curve to the right (Fig. 4*G*; two-way ANOVA for repeated measures over injection current, $F_{2,15} = 3.95$, $P < 0.05$), suggesting reduced neuronal excitability of VTA DA neurons after JWH133 application.

CB_2Rs Modulate DA Neuronal Activity in ex Vivo VTA Slices. We also tested the effects of JWH133 on VTA DA neuronal firing in VTA slice preparations using cell-attached patch-clamp recording techniques. In this recording mode, the intracellular environment of the recorded neurons is not interrupted. Fig. 4*H* shows representative records of VTA DA neuronal firing, illustrating that JWH133 significantly reduced VTA DA neuronal firing in VTA slices. Fig. 4*I* shows pooled data, illustrating that JWH133 and GW405833 significantly inhibited neuronal firing in a dose-dependent manner in WT mice (**$P < 0.01$, paired *t* test). This effect was blocked by AM630 (1 μM) and was absent in $CB_2^{-/-}$ mice.

We also examined the effects of JWH133 on GABA neuronal firing in VTA slices prepared from mice expressing GFP under the control of the GAD67 promoter (GAD67-GFP knock-in mice) (32) (Fig. S6). We found that, unlike VTA DA neurons, VTA GABA neurons (labeled by GFP) were insensitive to JWH133 (1, 10 μM) under the same experimental conditions (Fig. S6 *D*, *c*; $F_{3,36} = 0.85$, $P > 0.05$), suggesting that CB_2Rs predominantly modulate VTA DA, but not GABA, neuronal function.

CB_2Rs Modulate VTA DA Neuronal Firing in Vivo. To determine whether the effects observed in ex vivo cells and brain slices can be seen in vivo, we examined the effects of systemic administration of JWH133 on VTA DA neuronal firing in anesthetized mice using single-unit recording techniques. The criteria for identification of DA neurons in vivo were the same as we reported previously (33, 34). Fig. 5*A* shows the recording sites as revealed by histological examination after completion of electrophysiological recording. Fig. 5*B* shows a representative extracellular recording, illustrating that systemic administration of JWH133 (10 or 20 mg/kg i.p.) dose-dependently inhibited the basal FR and burst firing (BS) rate (defined as the number of burst spikes/s) in VTA DA neurons. This effect was reversed by systemic administration

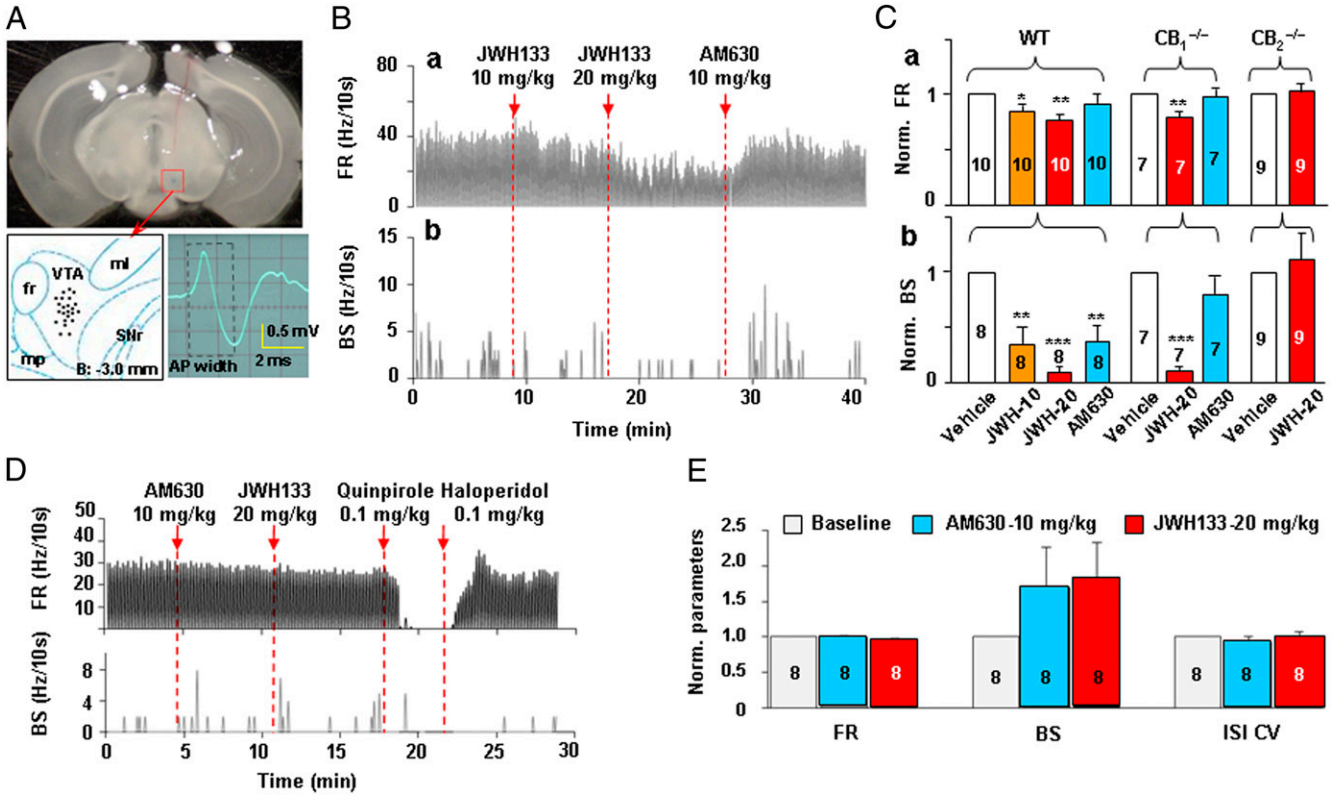

Fig. 5. CB_2R activation inhibits VTA DA neuronal firing in vivo. (*A*) Brain section image illustrating the track of a recording electrode and tips (recording sites) of the electrodes in the brain, and a characteristic action potential in a VTA DA neuron. (*B*) Representative extracellular single unit recording illustrating that JWH133 (10 or 20 mg/kg i.p.) dose-dependently inhibited basal FR and BS of VTA DA neurons in an anesthetized WT mouse. This effect was reversed by AM630 (10 mg/kg) administered 10 min after JWH133 injection. (*C*) Normalized FRs over the pre-JWH133 baseline, illustrating that JWH133 dose-dependently inhibited VTA DA neuronal firing in WT and $CB_1^{-/-}$ mice, but not in $CB_2^{-/-}$ mice. (*D* and *E*) Representative single-unit recording and summarized data illustrating that AM630 (10 mg/kg) alone failed to alter basal FR or ISI CV, but slightly potentiated BS. AM630 pretreatment prevented 20 mg/kg JWH133-induced inhibition of neuronal firing. Subsequent administration of quinpirole (a DA D_2R agonist, 0.1 mg/kg) inhibited VTA DA neuronal firing, which was reversed by haloperidol (a D_2R antagonist, 0.1 mg/kg). All quantificated data are normalized to control. Error bars indicate ± SEM. *$P < 0.05$; **$P < 0.01$; ***$P <$ 0.001 compared with predrug controls.

of 10 mg/kg AM630. Fig. 5*C* shows normalized FRs over pre-JWH133 baselines, illustrating that JWH133 significantly inhibited VTA DA neuronal firing in WT and $CB_1^{-/-}$ mice, but not in $CB_2^{-/-}$ mice. One-way ANOVA for repeated measures over JWH133 doses revealed a significant JWH133 treatment main effect on basal FR and BS in WT mice ($F_{3,27} = 5.07$, $P < 0.001$ and $F_{3,27} = 6.65$, $P < 0.01$, respectively) and in $CB_1^{-/-}$ mice ($F_{2,12} = 6.35$, $P < 0.05$ and $F_{2,12} = 6.87$, $P < 0.05$), but not in $CB_2^{-/-}$ mice (Fig. 5 *C*, *a* and *b*). In addition, JWH133 also significantly decreased the interspike interval coefficient of variation (ISI CV) in WT mice (from pre-JWH133 baseline of 1.0 ± 0 to 0.84 ± 0.04 after 10 mg/kg JWH133 or to 0.83 ± 0.03 after 20 mg/kg JWH133; $F_{3,36} = 4.03$, $P < 0.05$), suggesting a significant alteration in the burst firing pattern of VTA DA neurons after JWH133 administration (35).

We note that the inhibitory effect produced by JWH133 on burst firing was not completely reversed by AM630 administered after JWH133 (Fig. 5 *C*, *b*). Therefore, we further examined the effects of AM630 pretreatment on JWH133's action in VTA DA neurons. We found that pretreatment with AM630 (10 mg/kg) completely prevented JWH133-induced reduction in basal FR, burst firing, and ISI CV (Fig. 5 *D* and *E*), suggesting CB_2R-mediated effects. In addition, AM630 alone slightly enhanced burst firing (Fig. 5*E*), but this enhancement was not statistically significant compared with the pre-AM630 baseline ($F_{2,21} = 0.50$, $P > 0.05$).

CB_2Rs in the VTA Modulate Cocaine Self-Administration. Finally, we investigated whether activation of CB_2Rs in the VTA alters DA-regulated behavior. VTA DA neurons play a critical role in the rewarding effects of cocaine (28); thus, we examined whether microinjection of JWH133 into the VTA alters i.v. cocaine self-administration. In this experiment, 12 WT and 12 $CB_2^{-/-}$ mice were allowed daily cocaine self-administration. After 3–4 wk of daily access to cocaine (0.5 mg/kg for 3 h), most of the WT (9 of 12) and $CB_2^{-/-}$ mice (8 of 12) had acquired stable cocaine self-administration, defined as (*i*) at least 20 infusions per 3-h session, (*ii*) <20% variability in daily cocaine infusions across two consecutive sessions, and (*iii*) an active/inactive operant response ratio exceeding 2:1 (22, 36).

We found that bilateral microinjections of JWH133 (1 or 3 μg/1 μL/side) into the VTA (Fig. 6 *A*, *a*) significantly reduced cocaine self-administration in WT mice, but not in $CB_2^{-/-}$ mice (Fig. 6 *A*, *b* and *c*). This effect was blocked by coadministration of AM630 and JWH133, whereas microinjections of AM630 alone had no effect on cocaine self-administration. One-way ANOVA for repeated measures over dose revealed a significant JWH133 treatment main effect in WT mice ($F_{2,16} = 4.83$, $P < 0.05$), but not in $CB_2^{-/-}$ mice ($F_{2,14} = 0.81$, $P > 0.05$) (Fig. 6 *A*, *c*). In contrast, bilateral microinjections of the same doses of JWH133 into the VTA failed to alter oral sucrose self-administration (Fig. 6 *A*, *d*). Furthermore, bilateral microinjections of the same doses of JWH133 into a brain region adjacent to but outside and dorsal to the VTA (Fig. 6 *B*, *a*) had no effect on cocaine self-administration (Fig. 6 *B*, *b*). These results suggest that activation of VTA CB_2Rs selectively modulates cocaine, but not food, self-administration behavior.

Discussion

The major findings of the present study can be summarized as follows: (*i*) qRT-PCR detected low levels of CB_2 mRNA in several brain regions; (*ii*) ISH and IHC assays detected CB_2 mRNA and receptor expression in VTA DA neurons; (*iii*) activation of CB_2Rs by JWH133 or other CB_2 agonists inhibited VTA DA neuronal firing in single dissociated neurons, VTA slices, and anesthetized animals; (*iv*) microinjections of JWH133 into the VTA inhibited cocaine self-administration; and (*v*) all of the foregoing effects of JWH133 were blocked by CB_2R antagonism

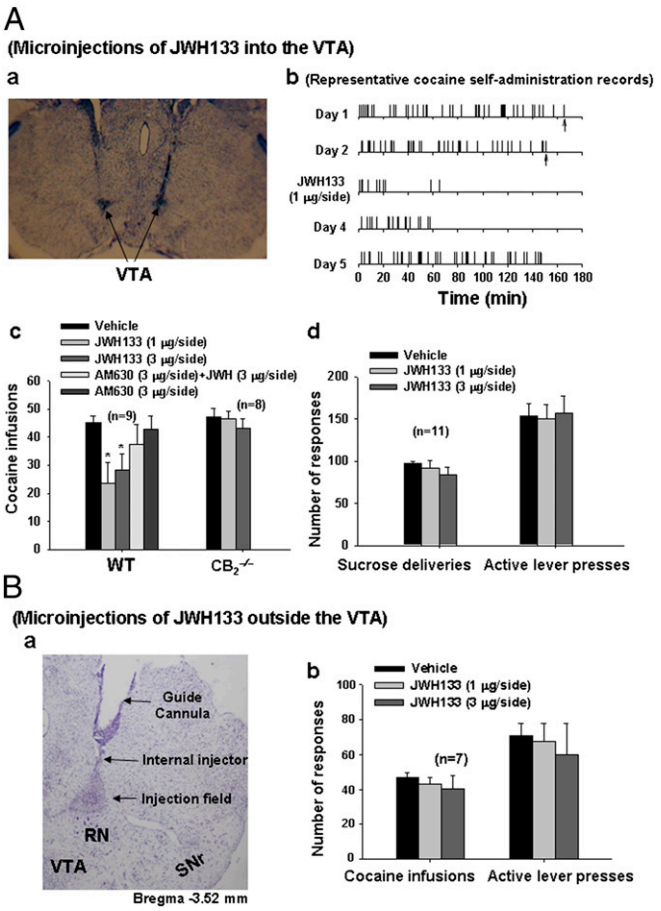

Fig. 6. Microinjections of JWH133 into the VTA inhibit i.v. cocaine self-administration. (*A*, *a*) Brain section image illustrating the track of representative guide cannulae and representative microinjection sites in the VTA. (*A*, *b* and *c*) Representative cocaine self-administration records and summarized data, illustrating that intra-VTA JWH133 microinjections significantly inhibit cocaine self-administration in WT mice, but not in $CB_2^{-/-}$ mice. (*A*, *d*) Bilateral microinjections of JWH133 into the VTA failed to alter oral sucrose self-administration behavior. (*B*, *a* and *b*) Microinjections of the same doses of JWH133 into a brain region adjacent and dorsal to the VTA (*B*, *a*) had no effect on cocaine self-administration (*B*, *b*). Up arrows indicate the last cocaine infusion allowed. All quantificated data are means ± SEM. **P* < 0.05, compared with vehicle group. RN, red nucleus; SNr, substantia nigra pars reticulata.

or absent in $CB_2^{-/-}$ mice. Taken together, these findings from genes to behavior provide convincing evidence that brain CB_2Rs are expressed in VTA DA neurons, where they modulate DA neuronal function and DA-regulated behavior.

CB_2 mRNA Is Expressed in Mouse Brain. Although growing evidence now suggests the presence of CB_2Rs in brain, conclusive evidence has been lacking owing to a lack of $CB_2^{-/-}$ mice and other necessary controls. Thus, whether functional CB_2Rs are expressed in VTA DA neurons has been unclear. To fully address these issues, we used multiple experimental approaches to study CB_2R expression and function in VTA DA neurons. We first used qRT-PCR to detect CB_2 mRNA expression in the brains of WT, $CB_1^{-/-}$, and $CB_2^{-/-}$ mice. We found that three different probes (CB_{2A}, CB_{2B}, and CB_2-KO probes) detected CB_2 mRNA in the brains of WT mice. The findings in $CB_2^{-/-}$ mice depended on the probes used. When we used probes targeted at the CB_2R gene sequences upstream and downstream from the region, the CB_2 mRNA signal was consistently detectable, whereas when we used a probe targeting the gene-deleted region, no CB_2 mRNA signal was detected.

These findings suggest that the $CB_2^{-/-}$ mice used in this study are actually partial, not full, knockouts in gene structure. Although these animals lack functional CB_2Rs, the majority of the CB_2 gene sequence is still present; thus, extreme caution is required when addressing CB_2 signaling specificity using such $CB_2^{-/-}$ mice as controls.

We note that brain CB_{2A} and CB_{2B} mRNA levels are very low compared with that in CB_2-rich spleen (~60-fold lower for CB_{2A} mRNA and ~500-fold lower for CB_{2B} mRNA in cortex than in spleen). This may explain why earlier ISH and RT-PCR studies failed to detect brain CB_2 mRNA, given that the experimental conditions used to detect high-density CB_2 mRNA in spleen might not be optimal for detecting low levels of CB_2 mRNA in the brain. Low densities of CB_2 mRNA in brain do not necessarily mean low levels of CB_2R expression, however. For example, brain opioid receptor mRNA levels are generally very low, particularly in the cerebral cortex, olfactory bulb, and spinal cord (37, 38); however, high densities of opioid receptors are expressed in those brain regions (37, 39). Because the CB_2-KO probe targeting the gene-deleted region in $CB_2^{-/-}$ mice detected CB_2 mRNA in WT and $CB_1^{-/-}$ mice, but not in $CB_2^{-/-}$ mice, we posit that the mRNA signaling detected by this probe is mCB_2-specific.

CB_2 mRNA Is Expressed in VTA DA Neurons. The foregoing findings with the CB_2-KO probe led us to successfully develop a mCB_2-specific riboprobe that allowed us to use the $CB_2^{-/-}$ mice as a negative control for studying CB_2 gene expression in VTA DA neurons. Using this probe, which also targets the gene-deleted region in $CB_2^{-/-}$ mice, we found that CB_2 mRNA is expressed in VTA neurons in WT and $CB_1^{-/-}$ mice, but not in $CB_2^{-/-}$ mice. This is consistent with the foregoing findings from qRT-PCR. Furthermore, double-label CB_2 mRNA assays (by ISH) and TH assays (by IHC) detected a low-to-moderate density of CB_2 mRNA staining in TH-positive VTA DA neurons in WT mice, but not in $CB_2^{-/-}$ mice, suggesting that CB_2R mRNA is natively expressed in mouse VTA DA neurons.

To further explore these findings, we successfully developed another riboprobe (CB_2 RNAscope probe) that allowed us to readily detect very low levels of CB_2 mRNA in the VTA and other brain loci. This probe is mCB_2-specific because it is a long riboprobe with 943 base pairs (*SI Experimental Procedures*) and targets a 3′ UTR sequence of the mCB_2 gene that shows no homology with CB_1 or other genes in the nucleotide sequence (Advanced Cell Diagnostics). In addition, RNAscope ISH uses a unique double RNA-specific oligonucleotide probe design strategy; thus, the chance of such Z-Z probes binding nonspecifically next to each other is very low (40). Furthermore, the RNAscope technology uses a unique probe design strategy that allows simultaneous amplification of multiple target mRNA signals and suppression of background noise signals (40). Therefore, it is highly sensitive to very low levels of mRNA, even a single molecule, and thus is particularly suitable for detecting CB_2 mRNA expression in the brain. Using such a probe, we detected low-to-moderate CB_2 mRNA in VTA DA neurons. This is congruent with our findings from qRT-PCR (Fig. 1) and from ISH combined with IHC (Fig. 2*A*). This probe also apparently detected CB_2 mRNA signaling in $CB_2^{-/-}$ mice (Fig. 2*B*), targeting the downstream 3′ UTR as distinct from the upstream gene-deleted region. These congruent findings using two different ISH assays with two different probes strongly suggest that CB_2 mRNA is expressed in VTA DA neurons.

CB_2R Protein Is Expressed in VTA DA Neurons. To determine whether CB_2R proteins are expressed in VTA DA neurons, we used three strains of mice (WT, $CB_1^{-/-}$, and $CB_2^{-/-}$) and three different CB_2 antibodies (Abcam, Alomone, and NIH-5633) for CB_2 immunostaining. Similar patterns and densities of CB_2R immunostaining in VTA DA neurons were detected in WT and $CB_1^{-/-}$ mice; however, the findings in $CB_2^{-/-}$ mice depended on the epitope of the antibody. Both the NIH5633 and Alomone mCB_2 antibodies with epitopes at the receptor-deleted region in $CB_2^{-/-}$ mice detected much higher densities of CB_2R immunostaining in both VTA DA neurons and splenocytes in WT mice than in $CB_2^{-/-}$ mice, whereas the Abcam rCB_2 antibody with epitope at the intact N terminal of CB_2Rs detected similar densities of CB_2 immunostaining, supporting mCB_2-specificity of the detected signal. We note that both the NIH5633 and Alomone antibodies should not detect CB_2R immunostaining in $CB_2^{-/-}$ mice, because they target the receptor-deleted region; however, both antibodies detected weak immunostaining in both VTA and spleen cells in $CB_2^{-/-}$ mice, suggesting that they are not absolutely mCB_2R-specific.

It has been reported that CB_2Rs are expressed and up-regulated in microglia during neuroinflammation in humans (21, 41). Our experiments did not reveal obvious CB_2R immunostaining in glial cells in the VTA. To confirm this, we used a GFAP antibody and a CD11b antibody to label VTA astrocytes and microglia, respectively, and used LPS to stimulate glial cell proliferation. We observed only weak CB_2 immunostaining in GFAP-labeled astrocytes and no CB_2 immunostaining in CD11b-labeled microglia. These findings are consistent with previous reports that microglia and astrocytes may not express CB_2Rs in healthy rats and mice (14, 41–43). More studies are required to address it.

CB_2R Activation Inhibits VTA DA Neuronal Firing. To determine whether CB_2Rs expressed in VTA DA neurons are functional, we used electrophysiological methods to study the response(s) of VTA DA neurons to selective CB_2R ligands. We explored this at three levels: single dissociated DA neurons, DA neurons in VTA slices, and DA neurons in intact anesthetized mice. We found that systemic or local (bath) administration of JWH133 or any of the four other CB_2R agonists significantly inhibited VTA DA neuronal firing in a dose- or concentration-dependent manner in WT and $CB_1^{-/-}$ mice. This inhibitory effect was reversed by pharmacologic blockade of CB_2Rs (AM630) or was absent in $CB_2^{-/-}$ mice, suggesting a CB_2R-mediated effect. This finding is consistent with previous reports in which JWH133 or other CB_2R agonists inhibited spontaneous and evoked neuronal firing to noxious stimuli in spinal cord and thalamus (44–47) and inhibited excitatory neuronal firing in the prefrontal cortex (48). Thus, our electrophysiological data provide direct evidence demonstrating that the expressed CB_2Rs in VTA DA neurons are functional, and that activation of these receptors inhibits VTA DA neuronal firing and decreases VTA DA neuronal excitability.

Furthermore, we found little effect of JWH133 on neuronal firing in identified VTA GABA neurons using GAD67-GFP transgenic mice, apparently contrary to a previous report that CB_2R agonists inhibit GABAergic synaptic transmission in cerebral cortex (49). This finding may be related to different cellular distributions of CB_2Rs in different brain regions.

As noted above, the burst activity of VTA DA neurons has been associated with increased vulnerability to cocaine self-administration (50). Consequently, we investigated whether VTA CB_2R activation inhibits cocaine self-administration behavior. We found that microinjections of JWH133 into the VTA selectively decreased cocaine, but not sucrose, self-administration in WT and $CB_1^{-/-}$ mice, but not in $CB_2^{-/-}$ mice. In contrast, microinjections of the same doses of JWH133 into a dorsal brain region adjacent to the VTA failed to alter cocaine self-administration, suggesting an effect produced by activation of CB_2Rs in the VTA, not in adjacent structures. This is consistent with our previous findings that systemic or local administration of JWH133 into the nucleus accumbens inhibits cocaine self-administration (22), and that transgenic up-regulation of brain CB_2Rs attenuates cocaine self-administration and cocaine-induced increased locomotion (19). The present findings are also congruent with recent

reports that brain CB_2Rs have important roles in other DA-related functions and/or CNS disorders (12, 25, 51, 52).

In conclusion, the present study demonstrates that CB_2Rs are expressed in VTA DA neurons and functionally modulate DA neuronal excitability and DA-related behavior. Considering that midbrain DA neurons play important roles in brain reward, locomotion, cognition, motivation, and various goal-directed behaviors, our findings provide direct evidence supporting an important role for VTA CB_2Rs in these actions, as well as in DA-related neurologic disorders, such as drug addiction. Thus, brain CB_2Rs may constitute a new therapeutic target for treatment of such CNS disorders.

Experimental Procedures

Animals. Male WT, CB_1 receptor knockout ($CB_1^{-/-}$) (53), and $CB_2^{-/-}$ mice (6, 54) with C57BL/6J genetic backgrounds were bred at the National Institute on Drug Abuse. In some experiments, glutamate decarboxylase-67 (GAD67)-GFP knock-in mice on a CD-1 background (55) were used for recording VTA GABA neuronal firing. All experimental procedures were conducted in accordance with the National Research Council's Guide for the Care and Use of Laboratory Animals (56), and were approved by the National Institute on Drug Abuse's Animal Care and Use Committee. The animals used for the electrophysiology experiments were transferred from the National Institute on Drug Abuse and bred at the Barrow Neurological Institute. Experimental procedures carried out at the Barrow Neurological Institute were conducted in accordance with the National Research Council's Guide for the Care and Use of Laboratory Animals (56) and the Barrow Neurological Institute's Institutional Animal Care and Use Committee guidelines.

qRT-PCR. The qRT-PCR assay of brain CB_2 mRNA levels was performed as described previously (10). Because immune cells in blood contain a high density of CB_2Rs, all mice used for qRT-PCR were perfused transcardially with 30–50 mL 0.9% saline under deep anesthesia, to prevent contamination of brain tissue by blood cells. Then brain and spleen were removed, and the prefrontal cortex, striatum, and midbrain were dissected. Three specific CB_2 probes were used: a CB_{2A} probe that recognizes the conjunction region of encoding exons 1 and 3, a CB_{2B} probe that recognizes the conjunction region of exons 2 and 3, and a CB_2-KO probe that targets the gene-deleted region close to the 3′ end of exon 3 in $CB_2^{-/-}$ mice. Mouse β-actin mRNA served as an endogenous control. The specific base pair sequences of the minor groove binder (MGB)-TaqMan probes and the primers used to detect CB_2 and β-actin mRNAs are listed in Table S1.

ISH.

CB_2 ISH and TH IHC Assays. Total RNA was isolated from C57BL/6J mouse brain samples using the Qiagen RNeasy Mini Kit according to the manufacturer's protocol. cDNA was synthesized from total RNA using the Bio-Rad iScript cDNA Synthesis Kit. For CB_2-mRNA riboprobe synthesis, oligonucleotide primers were designed specifically to detect the deleted mCB_2 mRNA region in $CB_2^{-/-}$ mice: forward primer 5′-AGCTCGGATGCGGCTAGAC-3′ and reverse primer 5′-AGGCTGTGGCCCATGAGA-3′. The template cDNA sequence of CB_2Rs was obtained from GenBank (ncbi.nlm.nih.gov/).

RNAscope ISH Assays. Both the CB_2 and TH RNA probes were designed and provided by Advanced Cell Diagnostics (Hayward, CA). The CB_2-specific RNA probe was designed to detect the 3′ UTR (1877-2820 bp) of the *Mus Cnr2* mRNA sequence (NM_009377.1, C1 channel) (Fig. 2*B*, *a*). The TH RNA probe was designed to detect 483–1,603 bp of *Mus musculus* TH mRNA sequence (NM_009924.3, C2 channel). Complete experimental methods for CB_2-ISH assays, along with TH-IHC and RNAscope ISH assays, are described in *SI Experimental Procedures*.

IHC Assays. Three CB_2R antibodies were used to detect CB_2R expression in VTA DA neurons in WT, $CB_1^{-/-}$, and $CB_2^{-/-}$ mice. Complete experimental methods for IHC assays are described in *SI Experimental Procedures*.

Electrophysiology Studies. Standard electrophysiological methods were used to record VTA DA neuronal responses to selective CB_2R ligands in single dissociated VTA DA neurons (using perforated patch-clamp recording), in VTA slices (using cell-attached patch-clamp recording), and in anesthetized mice (using extracellular single-unit recording). Complete electrophysiological methods are described in *SI Experimental Procedures*.

Intravenous Cocaine Self-Administration. Animal surgery, cocaine or sucrose self-administration, and intracranial microinjection procedures were as described previously (22). In brief, after stable cocaine or sucrose self-administration was achieved, subjects randomly received one microinjected dose of intra-VTA JWH133 (1 or 3 μg/side), AM630 (3 μg/side), a mixed solution of AM630 (3 μg/side) and JWH133 (3 μg/side), or vehicle (Tocrisolve 100) 30 min before cocaine or sucrose self-administration. After each test, animals underwent an additional 3–5 d of self-administration until the baseline response rate was reestablished before the next dose was tested. Cannula placements were verified after completion of the experiments by standard histological and anatomic localization techniques.

Data Analyses. All data are presented as means ± SEM. One-way or two-way ANOVA (SigmaStat software) was used to analyze the significance of the effects of JWH133 or other drugs on neuronal firing and cocaine self-administration. Individual group comparisons were carried out using the Student Newman–Keuls method. In addition, paired *t* tests were used to analyze some electrophysiological data, as described previously (30, 31). FRs and burst firing were determined every 10 s, as described previously (57, 58).

ACKNOWLEDGMENTS. We thank Dr. Yavin Shaham for his critical reading and comments on the manuscript, Dr. Ken Mackie (Indiana University Bloomington) for advice and counsel during the performance of this research, and Dr. Scott Steffensen (Brigham Young University Provo) for providing GAD67-GFP transgenic mice. This research was supported by the Intramural Research Program of the National Institute on Drug Abuse, National Institutes of Health. The electrophysiological studies were supported by the Barrow Neuroscience Foundation (M.G.) and the Barrow Neurological Institute–Bristol-Myers Squibb Seed Fund (J.W.).

1. Munro S, Thomas KL, Abu-Shaar M (1993) Molecular characterization of a peripheral receptor for cannabinoids. *Nature* 365(6441):61–65.
2. Galiègue S, et al. (1995) Expression of central and peripheral cannabinoid receptors in human immune tissues and leukocyte subpopulations. *Eur J Biochem* 232(1): 54–61.
3. Griffin G, et al. (1999) Evaluation of the cannabinoid CB_2 receptor-selective antagonist, SR144528: Further evidence for cannabinoid CB_2 receptor absence in the rat central nervous system. *Eur J Pharmacol* 377(1):117–125.
4. Schatz AR, Lee M, Condie RB, Pulaski JT, Kaminski NE (1997) Cannabinoid receptors CB_1 and CB_2: A characterization of expression and adenylate cyclase modulation within the immune system. *Toxicol Appl Pharmacol* 142(2):278–287.
5. McCoy KL, Matveyeva M, Carlisle SJ, Cabral GA (1999) Cannabinoid inhibition of the processing of intact lysozyme by macrophages: Evidence for CB_2 receptor participation. *J Pharmacol Exp Ther* 289(3):1620–1625.
6. Buckley NE, et al. (2000) Immunomodulation by cannabinoids is absent in mice deficient for the cannabinoid CB(2) receptor. *Eur J Pharmacol* 396(2-3):141–149.
7. Lu Q, Straiker A, Lu Q, Maguire G (2000) Expression of CB_2 cannabinoid receptor mRNA in adult rat retina. *Vis Neurosci* 17(1):91–95.
8. Skaper SD, et al. (1996) The ALIAmide palmitoylethanolamide and cannabinoids, but not anandamide, are protective in a delayed postglutamate paradigm of excitotoxic death in cerebellar granule neurons. *Proc Natl Acad Sci USA* 93(9):3984–3989.
9. Lanciego JL, et al. (2011) Expression of the mRNA coding the cannabinoid receptor 2 in the pallidal complex of *Macaca fascicularis*. *J Psychopharmacol* 25(1):97–104.
10. Liu QR, et al. (2009) Species differences in cannabinoid receptor 2 (CNR2 gene): Identification of novel human and rodent CB_2 isoforms, differential tissue expression and regulation by cannabinoid receptor ligands. *Genes Brain Behav* 8(5): 519–530.
11. Garcia-Gutierrez MS, Garcia-Bueno B, Zoppi S, Leza JC, Manzanares J (2011) Chronic blockade of cannabinoid CB(2) receptors induces anxiolytic-like actions associated to alterations in GABA(A) receptors. *Br J Pharmacol* 165(4):951–64.
12. Navarrete F, Pérez-Ortiz JM, Manzanares J (2012) Cannabinoid CB_2 receptor-mediated regulation of impulsive-like behaviour in DBA/2 mice. *Br J Pharmacol* 165(1): 260–273.
13. Van Sickle MD, et al. (2005) Identification and functional characterization of brainstem cannabinoid CB_2 receptors. *Science* 310(5746):329–332.
14. Viscomi MT, et al. (2009) Selective CB_2 receptor agonism protects central neurons from remote axotomy-induced apoptosis through the PI3K/Akt pathway. *J Neurosci* 29(14):4564–4570.
15. Ashton JC, Friberg D, Darlington CL, Smith PF (2006) Expression of the cannabinoid CB_2 receptor in the rat cerebellum: An immunohistochemical study. *Neurosci Lett* 396(2):113–116.
16. Baek JH, Zheng Y, Darlington CL, Smith PF (2008) Cannabinoid CB_2 receptor expression in the rat brainstem cochlear and vestibular nuclei. *Acta Otolaryngol* 128(9):961–967.
17. Brusco A, Tagliaferro P, Saez T, Onaivi ES (2008) Postsynaptic localization of CB_2 cannabinoid receptors in the rat hippocampus. *Synapse* 62(12):944–949.
18. Gong JP, et al. (2006) Cannabinoid CB_2 receptors: Immunohistochemical localization in rat brain. *Brain Res* 1071(1):10–23.

19. Aracil-Fernández A, et al. (2012) Decreased cocaine motor sensitization and self-administration in mice overexpressing cannabinoid CB_2 receptors. *Neuropsychopharmacology* 37(7):1749–1763.
20. Schmidt W, Schäfer F, Striggow V, Fröhlich K, Striggow F (2012) Cannabinoid receptor subtypes 1 and 2 mediate long-lasting neuroprotection and improve motor behavior deficits after transient focal cerebral ischemia. *Neuroscience* 227:313–326.
21. Atwood BK, Mackie K (2010) CB_2: A cannabinoid receptor with an identity crisis. *Br J Pharmacol* 160(3):467–479.
22. Xi ZX, et al. (2011) Brain cannabinoid CB2 receptors modulate cocaine's actions in mice. *Nat Neurosci* 14(9):1160–1166.
23. Ignatowska-Jankowska BM, Muldoon PP, Lichtman AH, Damaj MI (2013) The cannabinoid CB_2 receptor is necessary for nicotine-conditioned place preference, but not other behavioral effects of nicotine in mice. *Psychopharmacology (Berl)* 229(4):591–601.
24. García C, et al. (2011) Symptom-relieving and neuroprotective effects of the phytocannabinoid Δ^9-THCV in animal models of Parkinson's disease. *Br J Pharmacol* 163(7): 1495–1506.
25. Ortega-Alvaro A, Aracil-Fernández A, García-Gutiérrez MS, Navarrete F, Manzanares J (2011) Deletion of CB_2 cannabinoid receptor induces schizophrenia-related behaviors in mice. *Neuropsychopharmacology* 36(7):1489–1504.
26. García-Gutiérrez MS, Manzanares J (2011) Overexpression of CB_2 cannabinoid receptors decreased vulnerability to anxiety and impaired anxiolytic action of alprazolam in mice. *J Psychopharmacol* 25(1):111–120.
27. García-Gutiérrez MS, Pérez-Ortiz JM, Gutiérrez-Adán A, Manzanares J (2010) Depression-resistant endophenotype in mice overexpressing cannabinoid CB(2) receptors. *Br J Pharmacol* 160(7):1773–1784.
28. Wise RA, Rompre PP (1989) Brain dopamine and reward. *Annu Rev Psychol* 40:191–225.
29. Xi ZX, Gardner EL (2008) Hypothesis-driven medication discovery for the treatment of psychostimulant addiction. *Curr Drug Abuse Rev* 1(3):303–327.
30. Wu J, et al. (2004) Electrophysiological, pharmacological, and molecular evidence for alpha7-nicotinic acetylcholine receptors in rat midbrain dopamine neurons. *J Pharmacol Exp Ther* 311(1):80–91.
31. Yang K, et al. (2009) Distinctive nicotinic acetylcholine receptor functional phenotypes of rat ventral tegmental area dopaminergic neurons. *J Physiol* 587(Pt 2):345–361.
32. Brown RE, et al. (2008) Characterization of GABAergic neurons in rapid-eye-movement sleep controlling regions of the brainstem reticular formation in GAD67-green fluorescent protein knock-in mice. *Eur J Neurosci* 27(2):352–363.
33. Gao M, et al. (2010) Mechanisms involved in systemic nicotine-induced glutamatergic synaptic plasticity on dopamine neurons in the ventral tegmental area. *J Neurosci* 30(41):13814–13825.
34. Zhang D, et al. (2012) Impact of prefrontal cortex in nicotine-induced excitation of ventral tegmental area dopamine neurons in anesthetized rats. *J Neurosci* 32(36): 12366–12375.
35. Shi WX (2005) Slow oscillatory firing: A major firing pattern of dopamine neurons in the ventral tegmental area. *J Neurophysiol* 94(5):3516–3522.
36. Song R, et al. (2012) Increased vulnerability to cocaine in mice lacking dopamine D3 receptors. *Proc Natl Acad Sci USA* 109(43):17675–17680.
37. Mansour A, et al. (1994) Mu, delta, and kappa opioid receptor mRNA expression in the rat CNS: An in situ hybridization study. *J Comp Neurol* 350(3):412–438.
38. Mansour A, Fox CA, Thompson RC, Akil H, Watson SJ (1994) Mu-opioid receptor mRNA expression in the rat CNS: Comparison to mu-receptor binding. *Brain Res* 643(1-2):245–265.
39. Mansour A, Fox CA, Burke S, Akil H, Watson SJ (1995) Immunohistochemical localization of the cloned mu opioid receptor in the rat CNS. *J Chem Neuroanat* 8(4): 283–305.
40. Wang F, et al. (2012) RNAscope: A novel in situ RNA analysis platform for formalin-fixed, paraffin-embedded tissues. *J Mol Diagn* 14(1):22–29.
41. Stella N (2010) Cannabinoid and cannabinoid-like receptors in microglia, astrocytes, and astrocytomas. *Glia* 58(9):1017–1030.
42. Stella N (2004) Cannabinoid signaling in glial cells. *Glia* 48(4):267–277.
43. Zhang J, et al. (2003) Induction of CB_2 receptor expression in the rat spinal cord of neuropathic but not inflammatory chronic pain models. *Eur J Neurosci* 17(12):2750–2754.
44. Elmes SJ, Jhaveri MD, Smart D, Kendall DA, Chapman V (2004) Cannabinoid CB_2 receptor activation inhibits mechanically evoked responses of wide dynamic range dorsal horn neurons in naïve rats and in rat models of inflammatory and neuropathic pain. *Eur J Neurosci* 20(9):2311–2320.
45. Jhaveri MD, et al. (2008) Evidence for a novel functional role of cannabinoid CB(2) receptors in the thalamus of neuropathic rats. *Eur J Neurosci* 27(7):1722–1730.
46. Nackley AG, Zvonok AM, Makriyannis A, Hohmann AG (2004) Activation of cannabinoid CB_2 receptors suppresses C-fiber responses and windup in spinal wide dynamic range neurons in the absence and presence of inflammation. *J Neurophysiol* 92(6): 3562–3574.
47. Sagar DR, et al. (2005) Inhibitory effects of CB_1 and CB_2 receptor agonists on responses of DRG neurons and dorsal horn neurons in neuropathic rats. *Eur J Neurosci* 22(2):371–379.
48. den Boon FS, et al. (2012) Excitability of prefrontal cortical pyramidal neurons is modulated by activation of intracellular type-2 cannabinoid receptors. *Proc Natl Acad Sci USA* 109(9):3534–3539.
49. Morgan NH, Stanford IM, Woodhall GL (2009) Functional CB_2 type cannabinoid receptors at CNS synapses. *Neuropharmacology* 57(4):356–368.
50. Marinelli M, White FJ (2000) Enhanced vulnerability to cocaine self-administration is associated with elevated impulse activity of midbrain dopamine neurons. *J Neurosci* 20(23):8876–8885.
51. Agudo J, et al. (2010) Deficiency of CB_2 cannabinoid receptor in mice improves insulin sensitivity but increases food intake and obesity with age. *Diabetologia* 53(12): 2629–2640.
52. Flake NM, Zweifel LS (2012) Behavioral effects of pulp exposure in mice lacking cannabinoid receptor 2. *J Endod* 38(1):86–90.
53. Zimmer A, Zimmer AM, Hohmann AG, Herkenham M, Bonner TI (1999) Increased mortality, hypoactivity, and hypoalgesia in cannabinoid CB_1 receptor knockout mice. *Proc Natl Acad Sci USA* 96(10):5780–5785.
54. Buckley NE (2008) The peripheral cannabinoid receptor knockout mice: An update. *Br J Pharmacol* 153(2):309–318.
55. Tamamaki N, et al. (2003) Green fluorescent protein expression and colocalization with calretinin, parvalbumin, and somatostatin in the GAD67-GFP knock-in mouse. *J Comp Neurol* 467(1):60–79.
56. Committee on Care and Use of Laboratory Animals (1996) *Guide for the Care and Use of Laboratory Animals* (Natl Inst Health, Bethesda), DHHS Publ No (NIH) 85-23.
57. Zhang D, Yang S, Jin GZ, Bunney BS, Shi WX (2008) Oscillatory firing of dopamine neurons: Differences between cells in the substantia nigra and ventral tegmental area. *Synapse* 62(3):169–175.
58. Gao M, et al. (2007) Functional coupling between the prefrontal cortex and dopamine neurons in the ventral tegmental area. *J Neurosci* 27(20):5414–5421.